A Chaotic Spiking Oscillator with a Pulse-Train Input

Keita Miyachi, Hidehiro Nakano and Toshimichi Saito

EEE Dept., Hosei Univ., 3-7-2, Kajino-cho, Koganei-shi, Tokyo, 184-8584, JAPAN
E-mail: {*miyachi*, *nakano*}@*nonlinear.k.hosei.ac.jp* , *tsaito@k.hosei.ac.jp*

Abstract

This paper studies a chaotic spiking oscillator (CSO) with a pulse-train input. The CSO has two continuous states and the pulse-train is non-equidistant. Applying the pulse-train input, it exhibits interesting synchronous and asynchronous phenomena to the input. The dynamics can be described by composite of 1-D return maps. Using the map, we analyze the response characteristic of the CSO.

1. INTRODUCTION

Pulse-coupled networks (ab. PCNs) of integrate-and-fire models (ab. IFMs) have been studied with great interests. The motivations for studying such models are including three points. First, the PCNs are basic nonlinear systems which exhibit interesting synchronization and bifurcation phenomena [1]-[4], [6][8]. Second, the PCNs are simple models to consider information processing function in the brain [4][8]. Third, the pulse-train dynamics is used effectively for efficient engineering applications such as associative memories [3][4][6]. In order to approach dynamics of the PCNs, it is fundamental to consider response characteristics of an IFM to pulse-train input(s). The IFM exhibits interesting synchronous and asynchronous phenomena [2], [4], and the pulse-train input is important to consider nonlinear analogs of the sampling theorem.

This paper studies a chaotic spiking oscillator (CSO) with a pulse-train input. The CSO consists of a linear 2-port voltage control current source(ab. 2PVCCS) and a firing switch. The operation of the firing switch is "the capacitor voltage v_1 reaches threshold voltage V_T or the pulse-train input is applied, the firing switch is closed and v_1 is reset to base voltage E instantaneously". Applying the pulse-train input, the CSO exhibits synchronous and asynchronous phenomena to the input. We consider the response characteristic for non-equidistant pulse-train input. However, the dynamics can be described by composite of 1-D return map. Using the map, we analyze the CSO's phenomena with non-equidistance pulse-train input. The case of equidistance pulse-train input is discussed in [5][7]

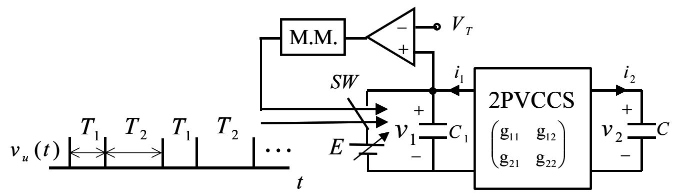

Figure 1: Chaotic Spiking Oscillator with pulse-train input

2. CHAOTIC SPIKING OSCILLATOR WITH PULSE-TRAIN INPUT

Fig. 1 shows the chaotic spiking oscillator with pulse-train input. In the figure 2PVCCS is a 2-port voltage-controlled current source characterized by four conductance parameters g_{11}, g_{12}, g_{21} and g_{22}. Connecting two capacitors to both ports of the 2PVCCS, we obtain a linear circuit described by

$$\frac{d}{dt}\begin{bmatrix} v_1 \\ v_2 \end{bmatrix} = \begin{bmatrix} g_{11}/C_1 & g_{12}/C_1 \\ g_{21}/C_2 & g_{22}/C_2 \end{bmatrix}\begin{bmatrix} v_1 \\ v_2 \end{bmatrix} \tag{1}$$

It corresponds to the case where the SW is opened. For convenience we assume that the coefficient matrix of Eq. (1) has unstable complex conjugate eigenvalues $\delta\omega \pm j\omega$:

$$\omega^2 = -\frac{g_{12}g_{21}}{C_1C_2} - \frac{1}{4}\left(\frac{g_{11}}{C_1} - \frac{g_{22}}{C_2}\right)^2 > 0,$$
$$\delta = \frac{1}{2\omega}\left(\frac{g_{11}}{C_1} + \frac{g_{22}}{C_2}\right) > 0.$$

Then, the circuit exhibits divergent vibration. The firing switch SW is closed by the following cases:
1) Self-firing (ab. SFR) occurs at the moment when the capacitor voltage v_1 reaches the threshold V_T.
2) Compulsory-firing (ab. CFR) occurs at the moment when the following periodic pulse-train input is applied:

$$v_u(t) = \begin{cases} V_H, & t = n(T_1+T_2) \text{ or } n(T_1+T_2)+T_1 \\ V_L, & \text{otherwise.} \qquad (n = 0,1,2,3....), \end{cases} \tag{2}$$

When SW is closed, the state v_1 is reset to the base voltage E instantaneously holding v_2 =constant.

$$(v_1(t^+), v_2(t^+)) = (E, v_2(t)),$$
$$\text{if } V_1(t) = V_T \text{ or } t = n(T_1+T_2),\ t = n(T_1+T_2)+T_1. \tag{3}$$

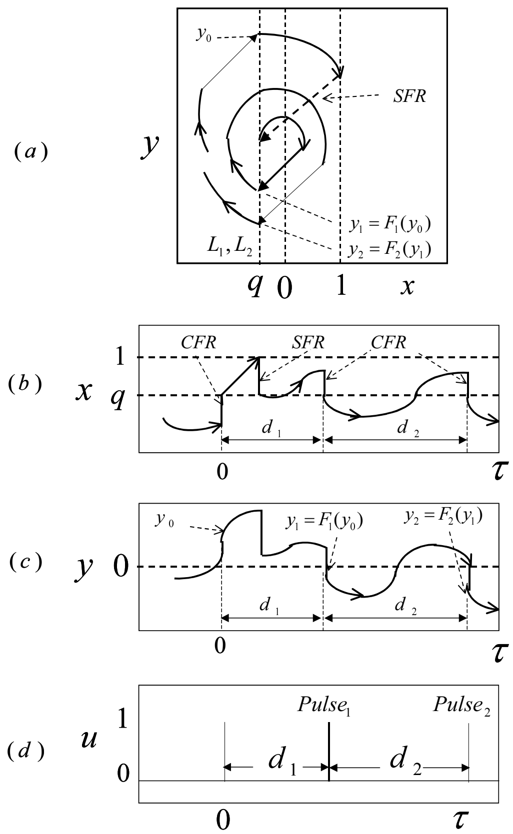

Figure 2: CSO with pulse-train input (a) Phase plane, (b) Time domain wave-forms of x, (c) Time domain wave-forms of y, (d) Pulse-train input

Using the dimensionless variables and parameters:

$$
\begin{aligned}
&\tau = \omega t,\ x = \frac{v_1}{V_T},\ \dot{x} = \frac{dx}{d\tau},\ y = \frac{1}{V_T}(pv_1 + \frac{g_{12}}{\omega C_1}v_2),\\
&p = \frac{1}{2\omega}(\frac{g_{11}}{C_1} - \frac{g_{22}}{C_2}),\ q = \frac{E}{V_T},\ d_1 = \omega T_1,\ d_2 = \omega T_2,
\end{aligned}
\tag{4}
$$

Equations (1) to (3) are transformed into Equations (5) to (7).

$$
\begin{bmatrix} \dot{x} \\ \dot{y} \end{bmatrix} = \begin{bmatrix} \delta & 1 \\ -1 & \delta \end{bmatrix} \begin{bmatrix} x \\ y \end{bmatrix},
$$

$$
\text{for } x < 1 \text{ and } \tau \neq n(d_1 + d_2) \text{ and } \tau \neq n(d_1 + d_2) + d_1, \tag{5}
$$

$$
(x(\tau^+), y(\tau^+)) = (q, y(\tau) - p(x(\tau) - q))
$$

$$
\text{if } x(\tau) = 1 \text{ or } \tau = n(d_1 + d_2) \text{ or } \tau = n(d_1 + d_2) + d_1 \tag{6}
$$

$$
u(\tau) = \begin{cases} 1, & \text{if } \tau = n(d_1 + d_2) \text{ or } \tau = n(d_1 + d_2) + d_1, \\ 0, & \text{otherwise.} \qquad \text{(n=0,1,2,3....)}, \end{cases} \tag{7}
$$

where $u(\tau)$ represents the normalized pulse-train input. This system is characterized by five parameters: the damping δ, the jumping slope p, the base q, and the normalized pulse intervals d_1 and d_2. For simplicity we fix $p = 1.0$, $q = -1.0$ and $\delta = 0.1$, and select d_1 and d_2 as control parameters. For $x < 1$, the exact piecewise solution of Eq. (5) is given by

$$
\begin{bmatrix} x(\tau) \\ y(\tau) \end{bmatrix} = e^{\delta\tau} \begin{bmatrix} \cos\tau & \sin\tau \\ -\sin\tau & \cos\tau \end{bmatrix} \begin{bmatrix} x(0) \\ y(0) \end{bmatrix}, \tag{8}
$$

3. 1-D Return Map

In order to derive the return map, we define $L_1 = \{(x, y, \tau) | x = q, (\tau = 0 \ mod \ (d_1 + d_2))\}$, $L_2 = \{(x, y, \tau) | x = q, (\tau = d_1 \ mod \ (d_1 + d_2))\}$ and let a point on L_q be represented by its y-coordinate. As shown in Fig. 2(a), the trajectory started from a point y_0 on L_q at $\tau = 0$. At $\tau = d_1$, the input causes the CFR_1 and the trajectory is reset to a point y_1 on L_q. Then we define the following 1-D return map:

$$
F_1 : L_1 \to L_2, \quad y_0 \mapsto y_1. \tag{9}
$$

In a likewise manner,

$$
F_2 : L_2 \to L_1, \quad y_1 \mapsto y_2. \tag{10}
$$

The return map from L_1 to L_1 is defined by the combination return map:

$$
F = F_1 \circ F_2 : L_1 \to L_1, \quad y_0 \mapsto y_2. \tag{11}
$$

If the Lyapunov exponent exists independently of the initial state, it is given by

$$
\lambda = \lim_{N\to\infty} \frac{1}{N} \sum_{n=0}^{N-1} \ln |DF(y_n)|, \tag{12}
$$

For almost all y_0, chaotic behavior is characterized by positiveness of the Lyapunov exponent. y_n and λ can be calculated using the exact piecewise solution (8).

A. d_1=d_2: equidistant pulse train

If $d \equiv d_1 = d_2$, the input pulse-train is equidistant. For such an input, CSO exhibits synchronous and asynchronous phenomena as shown in Fig. 3. If d increases, the CSO exhibits synchronous and asynchronous phenomena alternately as shown in Fig. 5(a). Fig. 5(b) shows Lyapunov exponent. For $\lambda < 0$, the CSO exhibits stable periodic synchronous phenomena. For $\lambda > 0$, the CSO exhibits chaotic asynchronous phenomena.

B. $d_1 \neq d_2$: non-equidistant pulse-train

If $d_1 \neq d_2$, the input pulse-train is non-equidistance. Bifurcation diagram and Lyapunov exponent are shown in Fig. 6. Chaotic asynchronous phenomena and periodic synchronous phenomena appear alternately, as shown in Fig. 6(a). If d_1 and d_2 vary, periodic phenomena characterized by $\lambda < 0$ exists in black region as shown in Fig 7.

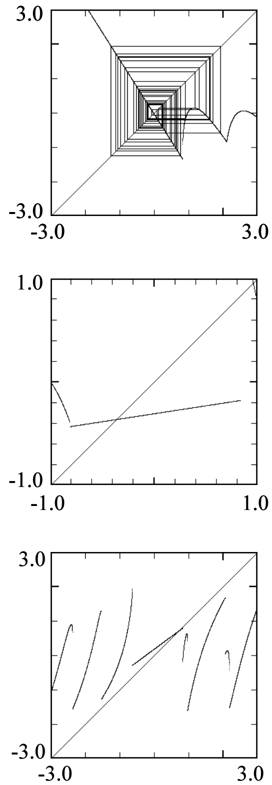

Figure 3: Typical return maps and corresponding attractors in the case of A:($\delta = 0.1, q = -0.1, p = 1.0, d = d_1 = d_2$)(a) $d = 2.0$, (b) $d = 4.0$, (c) $d = 6.8$

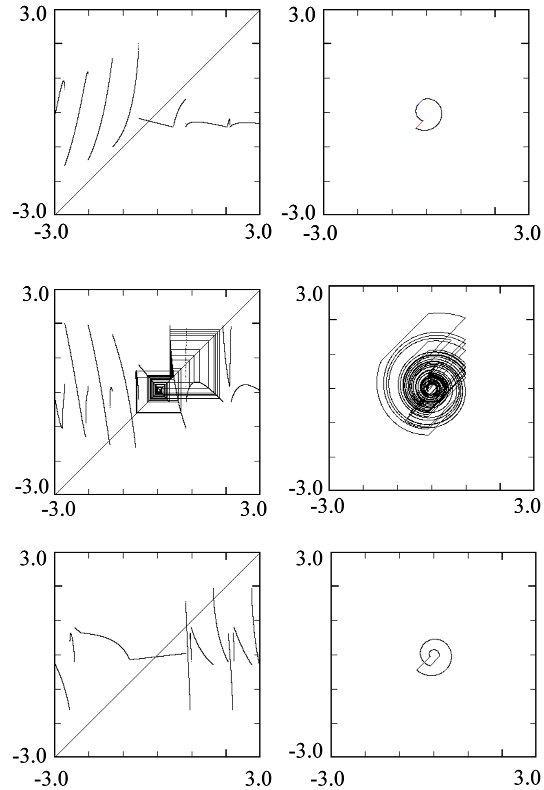

Figure 4: Typical return maps and corresponding attractors in the case of B:($\delta = 0.1, q = -0.1, p = 1.0$)(a) $d_1 = 2.0$, $d_2 = 4.0$, (b) $d_1 = 2.0$, $d_2 = 6.8$, (c) $d_1 = 4.0$, $d_2 = 6.8$

C. Non-periodic pulse-train

We consider the case where the input is non-periodic such that pulse interval is either d_1 or d_2 and each interval appears randomly and evenly. This case can be analyzed by a composite of F_1 and F_2 depending on appearance order of interval d_1 and d_2. Fig. 8 shows Lyapunov exponent. In Fig. 9, $\lambda < 0$ in the black region. We obtain similar result between the case of B and the case of C as shown in Fig. 7, 9.

4. CONCLUSION

We have studied response characteristics of CSO with pulse-train input. In order to analyze this CSO we use the composite return map. Using this map and Lyapunov exponent, we classify interesting synchronous and asynchronous phenomena. Preliminary results for non-periodic input have also been shown.

References

[1] J. P. Keener and F. C. Hoppensteadt & J. Rinzel, "Integrate-and-fire models of nerve membrane response to oscillatory input," *SIAM J. Appl. Math.,* 41, pp. 503-517, 1981.

[2] R. E. Mirollo & S. H. Strogatz, "Synchronization of pulse-coupled biological oscillators," *SIAM J. Appl. Math.,* 50, pp. 1645-1662, 1990.

[3] J. J. Hopfield & A. V. M. Herz, "Rapid local synchronization of action potentials: toward computation with coupled integrate-and-fire neurons," *Proc. Natl. Acad. Sci.,* 92, pp. 6655-6662, 1995.

[4] E. M. Izhikevich, "Weakly Pulse-coupled oscillators, FM Interactions, Synchronization, and oscillatory associative memory," *IEEE Trans. Neural Networks,* 10, 3, pp. 508-526, 1999.

[5] H. Nakano & T. Saito, "Basic dynamics from an integrate-and-fire chaotic circuit with a periodic input," *IEICE Trans. Fundamentals*, E84-A, 5. pp.1293-1300, 2001.

[6] H. Nakano & T. Saito, "Basic dynamics from a pulse-coupled network of autonomous integrate-and-fire chaotic circuits, *IEEE Trans. Neural Networks*, 13, 1, pp. 92-100, 2002.

[7] K. Miyachi, H. Nakano & T.Saito, "Responce characteristics of a chaotic spiking oscillator," *Proc IJCNN(2002).*

[8] E. M. Izhikevich, "Resonate-and-fire neurons," *Neural Networks,* 14, pp.883-894, 2001.

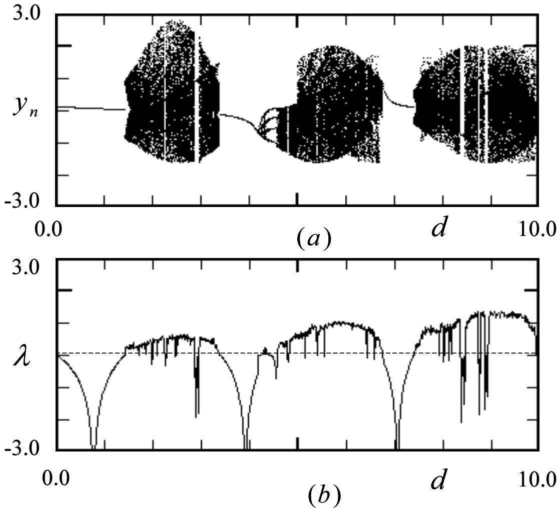

Figure 5: Response characteristic of CSO in the case of A: ($\delta = 0.1, p = 1.0, q = -0.1, d_1 = d_2$) (a)Bifurcation diagram, (b)Lyapunov exponent

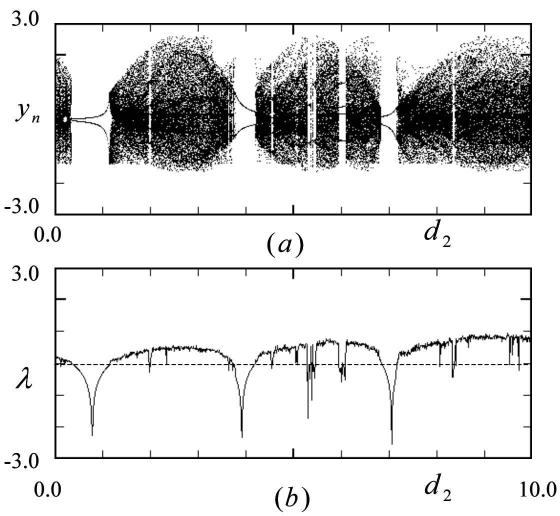

Figure 6: Response characteristic of CSO in the case of B: ($\delta = 0.1, p = 1.0, q = -0.1, d_1 = 2$) (a)Bifurcation diagram, (b)Lyapunov exponent

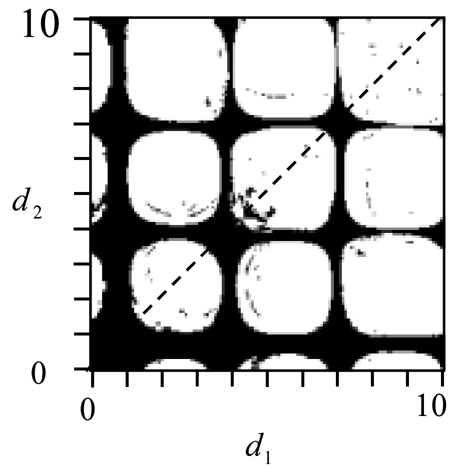

Figure 7: 3-D map of Lyapunov exponent in the case of B: ($p = 1.0, \delta = 0.1, q = -0.1$), $\lambda = 0.1$ for the white parts and $\lambda < 0$ for the black parts

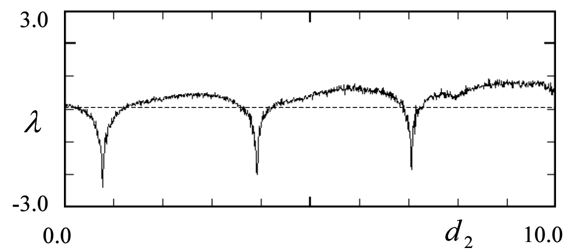

Figure 8: Lyapunov exponent in the case of C : ($\delta = 0.1, p = 1.0, q = -0.1, d_1 = 1.3$)

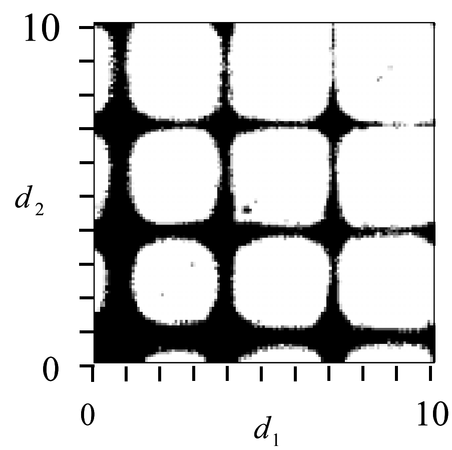

Figure 9: 3-D map of Lyapunov exponent in the case of C: ($p = 1.0, \delta = 0.1, q = -0.1$), $\lambda = 0.1$ for the white parts and $\lambda < 0$ for the black parts